Talanta 124 (2014) 139–145

Contents lists available at ScienceDirect

Talanta

journal homepage: www.elsevier.com/locate/talanta

A coumarin-derived fluorescent chemosensor for selectively detecting Cu^{2+}: Synthesis, DFT calculations and cell imaging applications

Fengjuan Chen [a,*], Guozhen Liu [b], Yanjun Shi [a], Pinxian Xi [a], Ju Cheng [c], Jinpeng Hong [c], Rong Shen [c], Xiaojun Yao [a], Decheng Bai [c], Zhengzhi Zeng [a,*]

[a] Key Laboratory of Nonferrous Metal Chemistry and Resources Utilization of Gansu Province, State Key Laboratory of Applied Organic Chemistry and College of Chemistry and Chemical Engineering, Lanzhou University, Lanzhou 730000, PR China
[b] Key Laboratory of Pesticide and Chemical Biology of Ministry of Education, College of Chemistry, Central China Normal University, Wuhan 430079, PR China
[c] School of Basic Medical Sciences, Lanzhou University, Lanzhou 730000, PR China

ARTICLE INFO

Article history:
Received 14 November 2013
Received in revised form
17 February 2014
Accepted 18 February 2014
Available online 25 February 2014

Keywords:
Chemosensor
Fluorescence
Live cell
Imaging
DFT
Cu^{2+}

ABSTRACT

A novel coumarin-based fluorescent probe L ((4E)-4-((7-hydroxy-4-methyl-2-oxo-2H-chromen-8-yl) methyleneamino)-1,2-dihyydro-2,3-dimethyl-1-phenylpyrazol-5-one) has been developed as a simple and efficient chemosensor which exhibits a significant fluorescence reduction in the presence of metal cations. This sensor exhibits high selectivity and sensitivity toward Cu^{2+} over other common cations. The mechanism for detecting copper was evaluated by time-dependent density functional theory (TD-DFT) calculations and the coordination mode was also confirmed by density functional theory (DFT) calculations. Furthermore, results of cell imaging in this study indicate that this new probe may be useful for detection and monitoring of Cu^{2+} in biological applications.

1. Introduction

A chemosensor is a molecule that renders a significant change in electronic, magnetic, or optical signals when it binds to a specific guest counterpart [1]. Among the various types of chemosensors, fluorescent chemosensors have several advantages over other methods due to their high sensitivity, intrinsic specificity, fast response, and real-time detection capabilities [2]. In recent years, great emphasis has been placed on the development of highly selective and rapidly specific chemosensors capable of monitoring heavy and transition metal ions (HTM), including Hg^{2+}, Zn^{2+}, and Cu^{2+}, due to their potential applications in clinical biochemistry and environmental research [3–6]. Sensors capable of detecting and measuring divalent copper is of particular interest. Cu^{2+} is the third most abundant soft transition metal ions in the human body after Fe^{2+} and Zn^{2+}. While Cu^{2+} plays a pivotal role in variety of fundamental physiological processes in organisms ranging from bacteria to mammals [7], excessive levels of copper can be toxic, and may cause oxidative stress and disorder associated with neurodegenerative diseases, including Menkes and Wilson diseases, familial amyotropic lateral sclerosis, Alzheimer's disease, and prion diseases [8].

In recent years, a number of fluorescent probes for Cu^{2+}-selective detection have been developed for biological applications [9]. However, many of these have exhibited limited applicability due to problems such as low sensitivity, high order of interference by co-existent metal ions, slow response, low fluorescence quantum yield in aqueous media or cytotoxicities of the ligand. Therefore, it is necessary to develop a new efficient chemosensor for Cu^{2+} detection which exhibits metal selectivity, high sensitivity with minimal sample manipulation, the ability to penetrate the cell membrane, structural and synthetic simplicity.

Coumarin and its derivatives are small organic molecules with excellent chromogenic and fluorogenic properties. These dyes are well known for their abilities to act as ion-detecting chemosensors. In this study, we have reported the synthesis of a new coumarin-derived Cu^{2+}-selective fluorescent sensor **L** bearing an ampyrone unit which exhibits a reversible "turn-off" fluorescent response for Cu^{2+} in aqueous medium with remarkably high sensitivity and selectivity. DFT calculations were used to evaluate the binding mode and fluorescence quenching mechanism of the sensor. Furthermore, bioimaging results indicated that this chemosensor can detect Cu^{2+} in living cells.

* Corresponding authors. Tel.: +86 931 8912596; fax: +86 931 8912582.
E-mail addresses: chenfj@lzu.edu.cn (F. Chen), zengzhzh@lzu.edu.cn (Z. Zeng).

http://dx.doi.org/10.1016/j.talanta.2014.02.034
0039-9140

2. Experimental

2.1. Instruments

^{1}H and ^{13}C NMR spectra were acquired on a Varian mercury-400 spectrometer with tetramethylsilane (TMS) as an internal standard and d^6-DMSO as solvent. Absorption spectra were determined on a Varian Cary 100 UV–vis spectrophotometer. Fluorescence spectra were measured on a Hitachi F-4500 spectrofluorimeter. Quantum yields were determined by an absolute method using an integrating sphere on an Edinburgh FLS920 Time Resolved Fluorescence Spectrometer. High Resolution Mass Spectroscopy (HRMS) data were acquired on a Bruker Daltonics APEXII 47e FT-ICR spectrometer.

2.2. Reagents and solutions

All materials for synthesis were purchased from commercial suppliers and used without further purification. HPLC grade acetonitrile without fluorescent impurities was used for spectra detection.

2.3. Synthesis of compound L

Compounds **1** (7-hydroxy-4-methyl-2H-chromen-2-one) and **2** (7-hydroxy-4-methyl-2-oxo-2H-chromen-8-carbaldehyde) were prepared according to the literature with minor modifications [10]. The reaction between resorcinol and ethylacetoacetate in ethanol at temperatures below 125 °C produced compound **1**, which was then treated with hexamine at 90–95 °C to synthesize compound **2**, a pale yellow solid. Subsequently, the probe **L** ((4E)-4-((7-hydroxy-4-methyl-2-oxo-2H-chromen-8-yl)methyleneamino)-1,2-dihyydro-2,3-dimethyl-1-phenylpyrazol-5-one) was easily synthesized via a three step procedure (Fig. 1). A mixture of compound **2** (0.0816 g, 0.4 mmol) and 4-aminoantipyrine (0.0813 g, 0.4 mmol) was refluxed in ethanol for 4 h. The target precipitate product was filtered from the yellow solution, washed with ethanol and dried over P_2O_5 under a vacuum to recover **L** as a yellow powder (80% yield). All of the newly synthesized products were well characterized by ^{1}H NMR, ^{13}C NMR, and ESI-MS (Supplementary materials, Figs. S9–S11). ^{1}H: NMR (d^6-$CDCl_3$, 400 MHz) δ (ppm): 14.945 (s, 1H), 10.293 (s, 1H), 7.468–7.505 (q, 3H), 7.381–7.402 (t, 2H), 7.318–7.355 (t, 1H, J=7.2 Hz), 6.818–6.840 (d, 1H, J=8.8 Hz), 6.071–6.073 (d, 1H, J=0.8 Hz), 3.218(s, 3H), 2.429 (s, 3H), 2.375 (s, 3H). ^{13}C NMR (d^6-$CDCl_3$, 50 MHz) δ (ppm): 164.49, 159.81, 159.76, 154.66, 153.88, 152.41, 149.63, 134.29, 129.26, 127.61, 127.24, 124.52, 116.01, 113.68, 111.58, 111.37, 108.03, 77.32, 77.00, 76.68, 35.61, 18.82, 10.32. ESI-MS (m/z)=390.3 $[M+H]^+$, calc. for $C_{22}H_{19}N_3O_4$=389.14.

A single crystal of **L** was obtained from a solution of CH_2Cl_2–CH_3OH (1:1, v/v), characterized using X-ray crystallography and allocated under deposition No. CCDC-861281(Fig. 2). The structure revealed close spatial proximity between the O3, O4 and N1 atoms, suggesting the potential for these three atoms to form a complex with metal ions. Therefore, probe **L** may act as a signal switcher which will turn off/on when the target cation is bound.

2.4. Procedures of metal ion sensing experiments

Stock solutions of the metal ions (1 mM) were prepared in deionized water. A stock solution of **L** (1 mM) was prepared in CH_3CN. The solution of **L** was then diluted to 10 μM with CH_3CN/water (95:5 v/v). In titration experiments, 2 mL of **L** (10 μM) was prepared in quartz optical cells of 1 cm optical path length. Aliquots of the Cu^{2+} stock solution were added to **L** using a micro-pipet. Spectral data were recorded at 2 min after the addition of Cu^{2+} stock solution. For selectivity experiments, samples were prepared by addition of metal ion stock solution into 2 mL **L** (10 μM) solution. All emission spectra were collected from 450 to 650 nm with excitation at 342 nm.

2.5. Cell culture

The HEP G2 cell line was provided by Institute of Biochemistry and Cell Biology (China). Cells were cultured in H-DMEM medium (Dulbecco's Modified Eagle's Medium, High Glucose), supplemented with 10% Fetal Bovine Serum (FBS) in an atmosphere of 5% CO_2, 95% air at 37 °C. Cells (5×10^8/L) were plated on 18 mm coverslips and allowed to adhere for 24 h. Experiments to assess the uptake of Cu^{2+} were carried out in the same medium, supplemented with

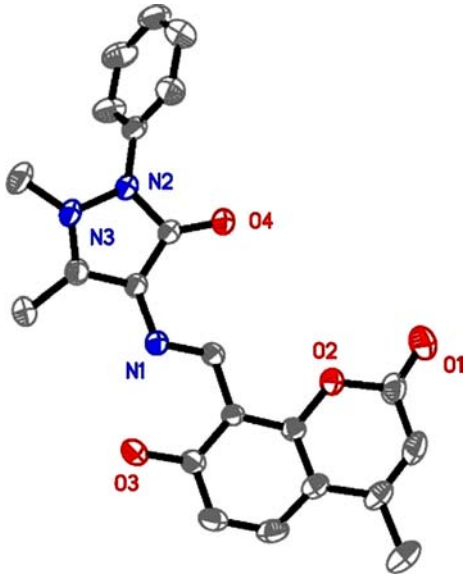

Fig. 2. The crystal structure of **L** with all hydrogen atoms omitted for clarity (50% probability level for the thermal ellipsoids).

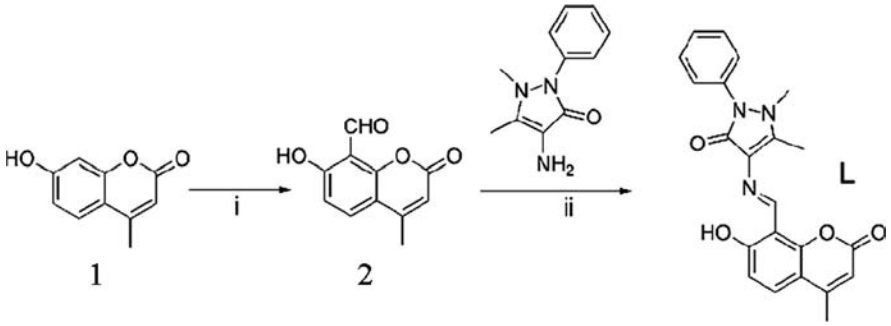

Fig. 1. The synthesis route of chemosensor **L**. Conditions: (i) Hexamine, HCl+water, at 94 °C; (ii) CH_3CH_2OH, reflux.

20 μM $CuCl_2$ after 2 h, and the cells were allowed to culture for 0.5 h.

2.6. Fluorescence imaging

Fluorescent pictures were taken on Zeiss Leica inverted epi-fluorescence/reflectance laser scanning confocal microscope. Excitation of L-loaded cells at 342 nm was carried out with a HeNe laser. Emissions were collected from 480 to 625 nm using a 520 nm long-pass filter. In these experiments, cells were initially washed with phosphate buffer saline (PBS) and then incubated with 10 μM **L** in DMSO–PBS (1:30, v/v) for 2 h at 37 °C. Cell imaging was then carried out after additional washing of the cells with PBS.

3. Results and discussion

3.1. Binding behavior of L toward Cu^{2+}

Fig. 3a shows the absorption data for **L** (10 μM) in CH_3CN/H_2O (95:5, v/v) following titration with Cu^{2+} (0–1 equiv.). Upon addition of Cu^{2+}, a new absorption band appeared at 416 nm concurrent with an increase in the intensity of the absorption bands centering at 338 nm. Additionally, the absorption bands concentrated at 243–341 nm and 379 nm were observed to decrease gradually with four isosbestic points at 243, 321, 357 and 389 nm. These phenomena implied that **L** and Cu^{2+} were coordinated, which resulted in the appearance of the new absorption in the longer wavelength region. A Job's plot depending on absorbance at 416 nm as a function of Cu^{2+} concentration was obtained (Fig. 3b), which indicated a 1:1 stoichiometry between **L** and Cu^{2+}, and this was further confirmed by the non-linear fitting of the UV–vis titration curve (Fig. 3c). It was also observed that the fluorescence intensity exhibited a linear increase with increasing concentration of Cu^{2+} over the range of 0–9 μM, with an estimated detection limit of 0.2 μM (Fig. 3d), which implied that this probe could be used for Cu^{2+} detection in blood [12].

3.2. Fluorescence response of L toward Cu^{2+}

In order to further investigate the binding mode between **L** and Cu^{2+}, a fluorescence titration was conducted and the data were evaluated using a Job's plot. Results of this experiment indicated a very strong luminescence (Φ_0=0.187) for **L** in CH_3CN/H_2O (95:5, v/v) solution. With the gradual addition of Cu^{2+} (0–1 equv.) into the solution of **L** (10 μM), the fluorescence intensity was quenched completely with an efficiency of 97.5% at 520 nm, and the quantum yield decreased to 0.098 (Fig. 4). Based on the maximum emission of **L**-Cu^{2+}, the fluorescence intensity of **L** exhibited a linear change relative to increasing concentration of Cu^{2+} between 0 and 10 μM, with a detection limit of 0.2 μM, which is consistent with the absorption results. These results further indicated that this sensor would be capable of determining the concentration of Cu^{2+} in blood [12]. Based on the fluorescence titration data, the association constant between **L** and Cu^{2+} was

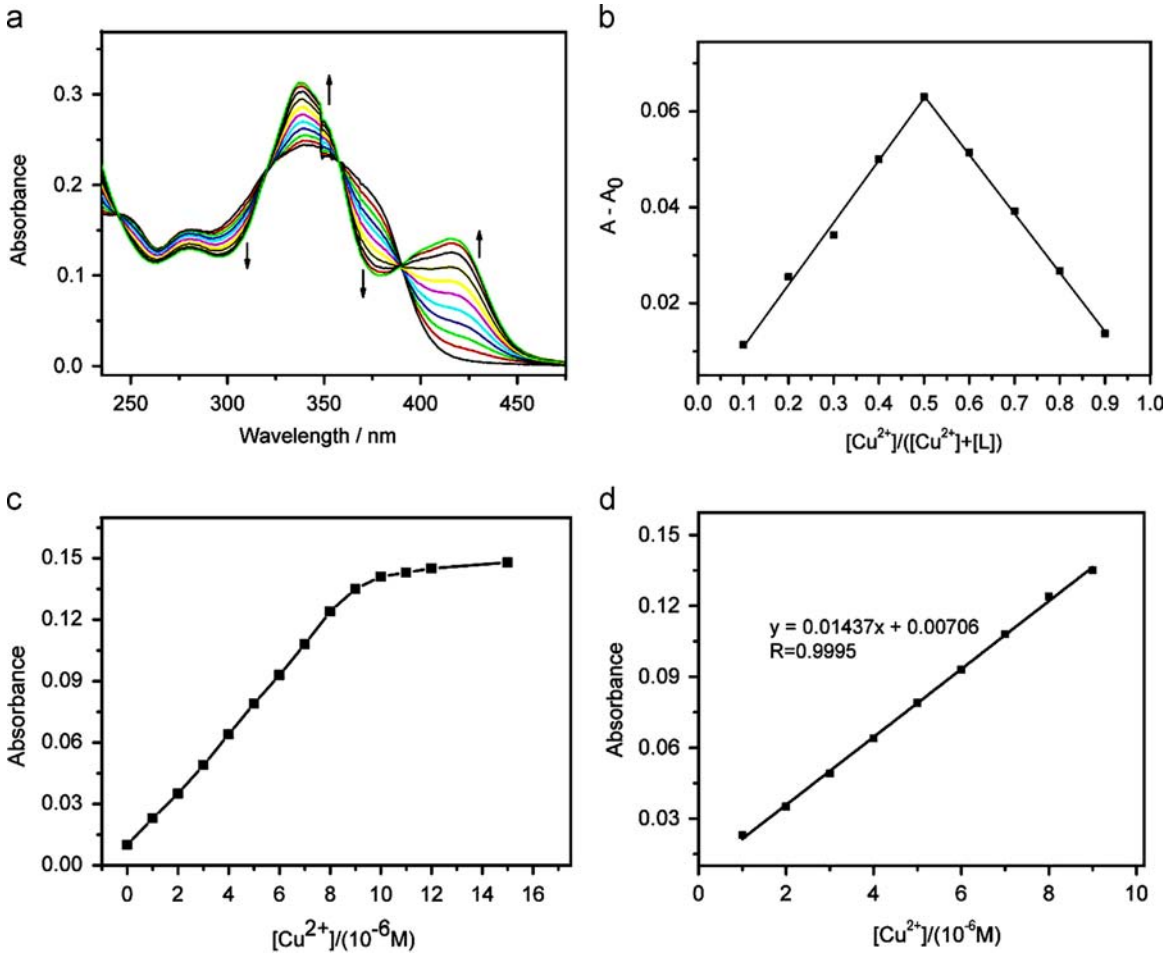

Fig. 3. (a) Absorbance spectra of **L** (10 μM) in CH_3CN/H_2O (95:5, v/v) following addition of Cu^{2+} (0–1 equiv.). (b) Job's plot according to the method for continuous variations (the total concentration of **L** and Cu^{2+} is 10 μM). (c) and (d) Absorbance of L (10 μM) at 416 nm as a function of Cu^{2+} (30 μM) concentration and the linear part.

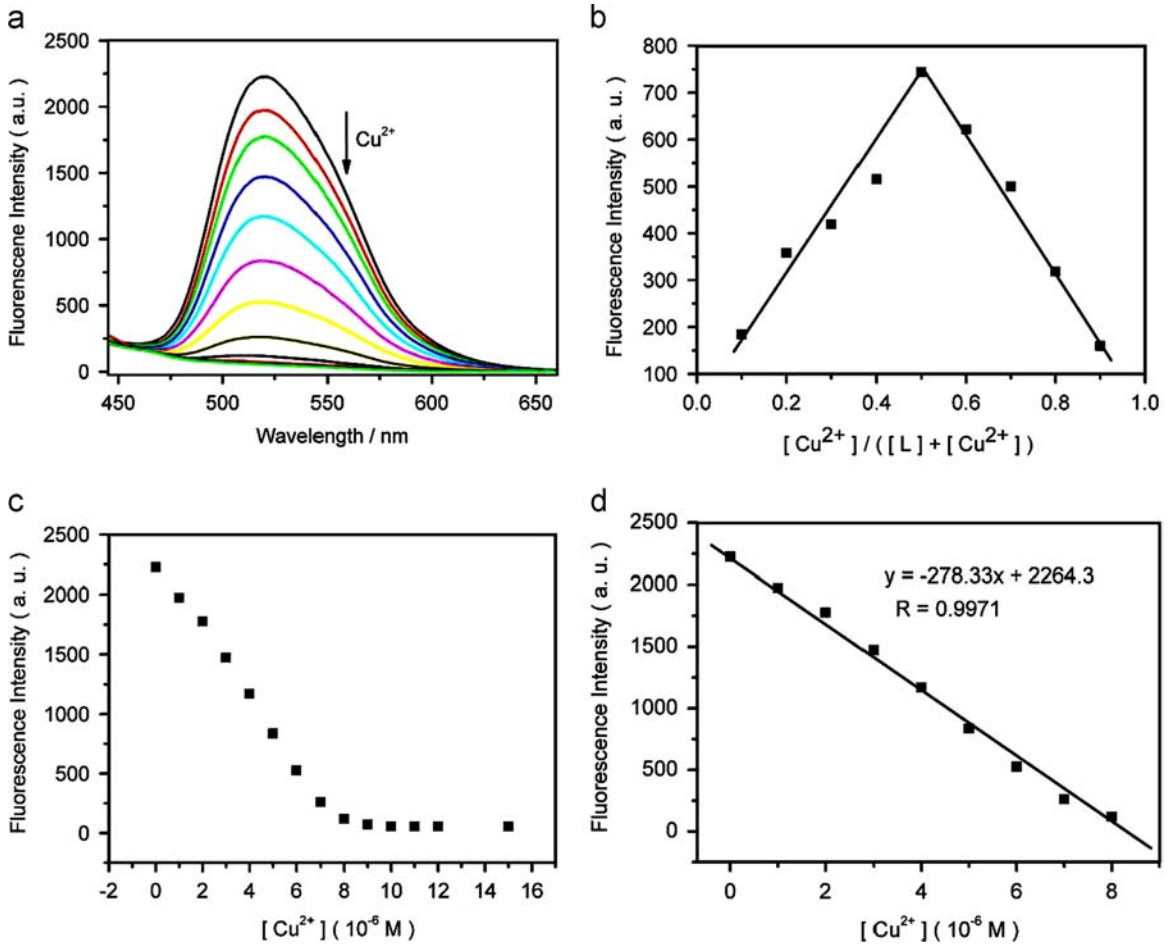

Fig. 4. (a) Fluorescence spectra of **L** (10 μM) following addition of Cu^{2+} (0–1 equiv.). (b) Job's plot according to the method for continuous variations (the total concentration of **L** and Cu^{2+} is 10 μM). (c) and (d) The fluorescence intensity of **L** (10 μM) at 520 nm as a function of Cu^{2+} (15 μM) concentration and the linear part (λ_{ex}=342 nm).

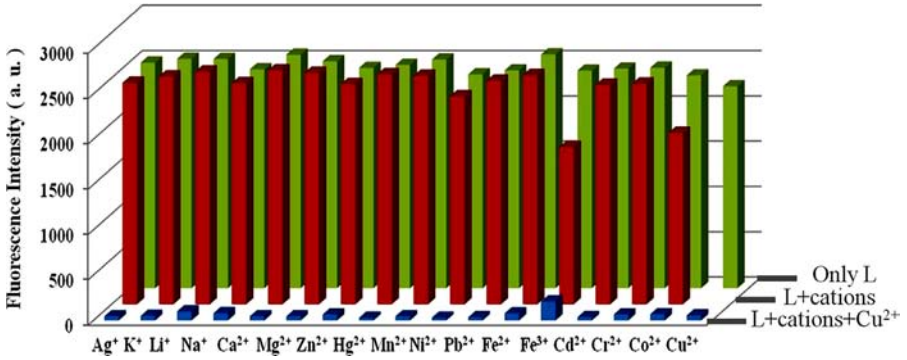

Fig. 5. Fluorescence emission intensities of **L** (10 μM) alone, **L** + various cations (10 μM) and **L** + cations + Cu^{2+} (10 μM) in CH_3CN/H_2O (95:5, v/v) solution, λ_{ex} = 342 nm.

calculated to be $\sim 6.57 \times 10^3\ M^{-1}$ (Fig. S1). Additionally, according to the non-linear fitting fluorescence titration curve, the binding mode between **L** and Cu^{2+} was revealed to be a 1: 1 stoichiometry, and this conclusion was further supported by analysis of Job's plot.

3.3. Selectivity

High selectivity for a specific analyte in the presence of competing species is another important feature of a chemosensor. To evaluate the selectivity of **L**, several additional metal ions including alkali, transition and alkali earth metal ions were tested under the same condition as the Cu^{2+}. Minimal changes in the absorption spectra was observed following the addition of Li^+, Na^+, K^+, Mg^{2+}, Ca^{2+}, Zn^{2+}, Cd^{2+}, Cr^{3+}, Hg^{2+}, Pb^{2+}, Ni^{2+}, Fe^{3+}, Fe^{2+}, Mn^{2+} and Ag^+, with a weak absorbance increase observed with addition of Co^{2+} (Fig. S2). Additionally, Cu^{2+} was the only ion evaluated that produced a significant fluorescence decrease, while other metal ions induced negligible fluorescence variations (Fig. S3). Moreover, the addition of Li^+, Na^+, K^+, Mg^{2+}, Ca^{2+}, Zn^{2+}, Cd^{2+}, Cr^{3+}, Hg^{2+}, Pb^{2+}, Ni^{2+}, Co^{2+}, Fe^{3+}, Fe^{2+}, Mn^{2+} and Ag^+ to **L** in the presence of Cu^{2+} did not influence the decrease in fluorescence intensity resulting from the addition of Cu^{2+}, thereby indicating that the interference of co-existent cations was negligible on the Cu^{2+} measurement (Fig. 5), even for K^+, Na^+, Mg^+

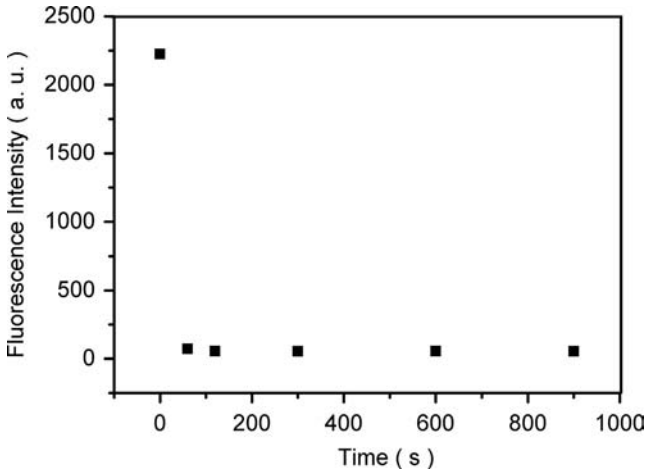

Fig. 6. Time course of the response of **L** (10 μM) to Cu^{2+} (10 μM) in CH_3CN/H_2O (95:5, v/v) solution.

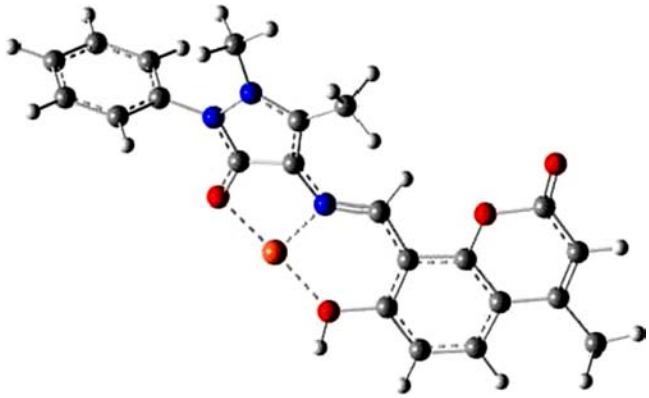

Fig. 7. Calculated energy-minimized structure of **L**–Cu^{2+}.

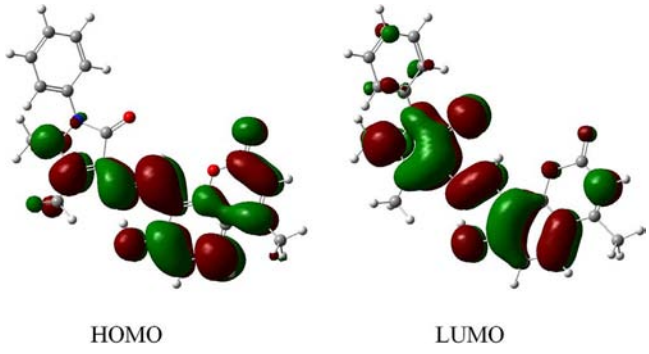

Fig. 8. Calculated HOMOs and LUMOs of **L**.

and Ca^{2+} at micromolar levels. As shown in Fig. 5, the addition of Fe^{3+} produced a marginal decrease in fluorescence intensity, but its fluorescence quenching effect toward **L** was far less than Cu^{2+} (Fig. S3). All of these results indicated that **L** is a good detection probe for Cu^{2+} ions with high selectivity and binding affinity. This chemosensor provides a strong signal-to-noise ratio under experimental conditions, suggesting the potential for wider use in practical applications.

To further evaluate and magnify the selectivity, and improve the sensitivity of probe **L**, the response of the **L**–Cu^{2+} system towards important physiological anions was investigated via absorbance and fluorescence spectra (Figs. S4–S5). The results revealed that S^{2-} could completely recover the absorbance and fluorescence intensity of the **L**–Cu^{2+} system at a 1:1 (**L**–Cu^{2+}: S^{2-},

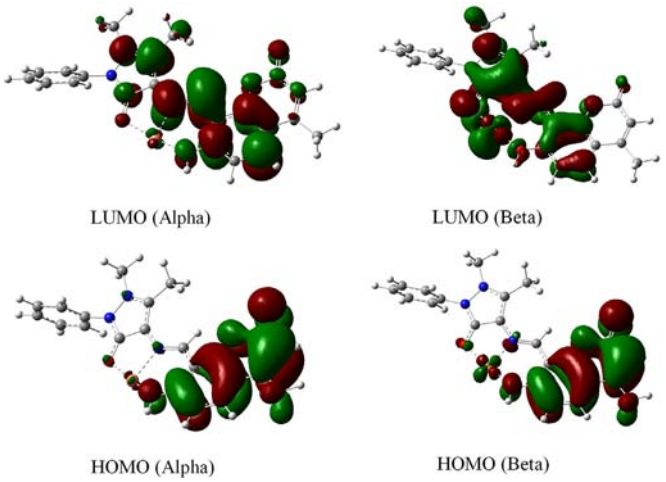

Fig. 9. Calculated HOMOs and LUMOs of **L**–Cu^{2+}.

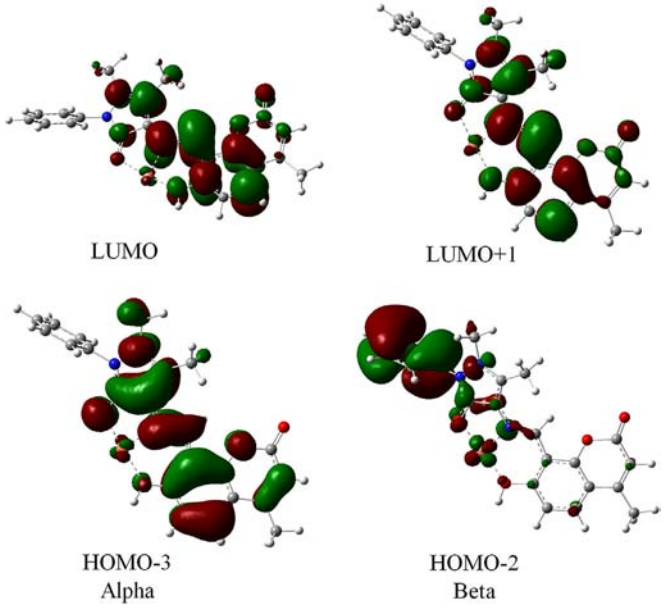

Fig. 10. Frontier molecular orbitals of **L**–Cu^{2+} relevant to the fluorescence quenching.

Table 1
The details of the contributions of orbital transitions for some electronic transitions with large oscillator strengths for L from the TD-DFT calculation.

	Percentage (%)	Excitation energy (nm)	Oscillator strength
Excited state 1:			
101 → 103	5.48	364.91 nm	f=0.4577
102 → 103	94.52		
Excited state 2:			
99 → 103	45.49	324.38 nm	f=0.1612
99 → 104	3.96		
100 → 103	4.05		
101 → 103	16.41		
102 → 104	30.09		
Excited state 3:			
99 → 103	22.84	305.28 nm	f=0.4057
100 → 103	65.67		
101 → 104	2.19		
102 → 104	9.30		

M/M) ratio, which further confirmed that the **L**–Cu^{2+} system comprised a 1:1 stoichiometry. It was also found that only S^{2-} (10 μM) could efficiently recover the fluorescence intensity of the **L**–Cu^{2+} system (10 μM), which was not observed with other anions, including F^-, Cl^-, Br^-, I^-, ClO^-, NO_3^-, CO_3^{2-}, HCO_3^-, SO_4^{2-}, HSO_4^-, HPO_4^-, CN^-, AcO^-, PO_4^{3-}, NO_2^-, $H_2PO_4^-$, MnO_4^- and HSO_3^-. One anion, $P_2O_7^{4-}$, did exhibited interference to a certain extent, but $P_2O_7^{4-}$ is not stable in aqueous medium (Fig. S6). These results indicated that the sensing of the **L**–Cu^{2+} system was hardly significantly altered in the presence of other common co-existent anions.

Table 2
The details of the contributions of orbital transitions for some electronic transitions with large oscillator strengths for L–Cu^{2+} system from the TD-DFT calculation. (A: Alpha, B: Beta).

	Percentage (%)	Excitation energy (nm)	Oscillator strength
Excited state 1:			
108A→112A	21.66	382.99 nm	f=0.2662
95B→111B	1.14		
96B→111B	1.11		
102B→111B	1.36		
105B→112B	2.69		
107B→112B	7.44		
108B→112B	64.60		
Excited state 2:			
104A→112A	1.13	376.23 nm	f=0.1892
108A→112A	16.10		
96B→111B	2.11		
99B→111B	1.72		
100B→111B	8.32		
101B→111B	1.76		
107B→112B	39.58		
108B→112B	29.28		

3.4. Response time

To evaluate the response time of the interaction between **L** and Cu^{2+}, the time course of the response of **L** (10 μM) was investigated in the presence of 1 equiv. of Cu^{2+} in CH_3CN/H_2O (95:5, v/v). An obvious spectra change was observed within 1 min (Fig. 6).

3.5. DFT calculations

To further evaluate the selectivity of **L** and confirm the complex formation of **L**–Cu^{2+}, DFT calculations with Becke's three parametrized Lee–Yang–Parr (B3LYP) exchange-correlation functional was carried out using the Gaussian 09 package. The 6-31G basis sets were used for the C, N, O atoms except for $Cu(NO_3)_2$, where the LANL2DZ effective core potential (ECP) was employed. The optimized configuration indicated the presence of three coordination bonds between Cu^{2+} and L, and the molecular system formed a nearly planar structure. The Cu–N bond length was 2.08217 Å, and the Cu–O bond lengths were 1.97838 Å (Cu–coumarin) and 1.97203 Å (Cu–aminoantipyrene). These data indicated that this semirigid structure could effectively provide adequate space to accommodate the corresponding metal ions.

In order to further understand the mechanism of the fluorescence quenching by the energy and/or charge transfer model,

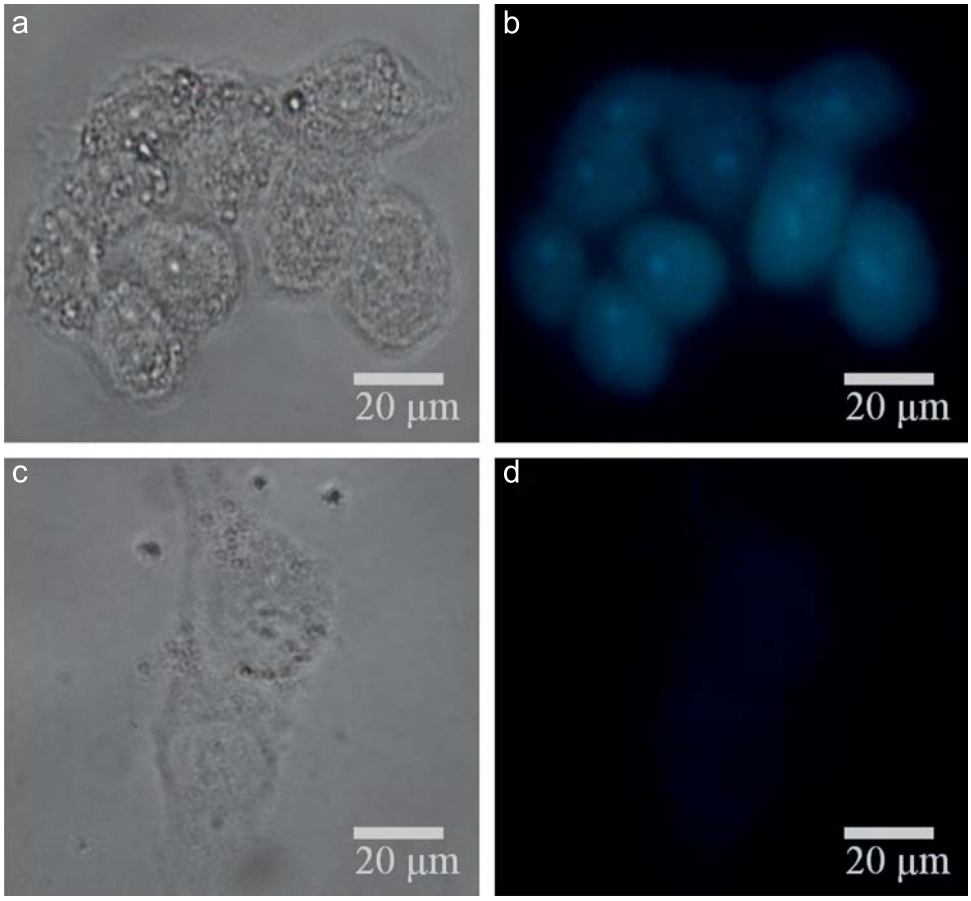

Fig. 11. Confocal fluorescence images of Cu^{2+} in Hep G2 cells (Zeiss LSM 510 META confocal microscope, 40× objective lens). (a) and (c) Brightfield image of Hep G2 cells. (b) Fluorescence image of Hep G2 cells incubated with **L** (10 μM). (d) Fluorescence image of Hep Cells incubated with 10 μM L for 0.5 h and further incubated with the addition of 10 equiv. $CuCl_2$ for 2 h at 37 °C.

TD-DFT calculations were performed at the optimized geometries (Figs. 7–10, Tables 1,2, more details in Supplementary materials Figs. S7,S8). From this calculation, we observed that the quenching mechanism could be rationalized in terms of the occupancy of the frontier orbitals. The HOMO to LUMO excitation of **L** was found to be relevant to charge transfer with a contribution of 94.5%. In the **L**–Cu complex, the molecular orbitals included both Alpha and Beta orbitals. The main transitions occurred from HOMO-3 to LUMO (Alpha orbital) and from HOMO-2 to LUMO+1 (Beta orbital), and their contributions to the lowest energy excitations were 21.7% and 64.6%, respectively. These results also revealed that the Beta orbital played a major role that was visible in the graphics of the orbitals. These excitations corresponded to charge transfer from the excited ampyrone moiety to the region surrounding the Cu^{2+} ion, and thus provided a pathway for nonradiative deactivation of the excited state. More detailed information regarding the atomic orbital contribution to specific frontier molecular orbitals, electronic energies and Cartesian coordinates are provided in Tables S1,S2 in the Supplementary materials.

3.6. Cell imaging

Since the ability of biosensing molecules to selectively monitor guest species in living cells is very important for biological applications [11–16], we proceeded to study the application of **L** as a Cu^{2+} probe in living cells (Fig. 11a–d). Considering the toxicity associated with Cu^{2+} accumulation in animals, we primarily performed experiments using **L** on liver cell lines in which Cu^{2+} was known to be accumulated. Hep G2 (liver cancer) cells displayed strong fluorescence (Fig. 11b) following incubation with 10 μM **L** for 20–30 min at 37 °C, which demonstrated that it was unaffected by intracellular quenchers, such as cell lysate. The treated cells were then washed with PBS buffer (pH 7.37) to remove the remaining **L**, and Cu^{2+} (10 equiv.) was added to the culture medium. After 2 h at 37 °C, the cells exhibited only very weak fluorescence (Fig. 11d). These results indicated that **L** can penetrate the cell membrane and is a suitable fluorescent probe for imaging and detection of Cu^{2+} in living cells.

4. Conclusions

In conclusion, we have developed a new coumarin derivate **L** which provides efficient tridentate coordination for Cu^{2+}. Results of absorbance and fluorescence titration experiments indicated that this new chemosensor can detect Cu^{2+} with high selectivity in the presence of other cations, and high sensitivity with a detection limit of 0.2 μM. Results of a Job's plot indicated a 1:1 coordination ratio between **L** and Cu^{2+}. The response time of **L** to Cu^{2+} was less than 1 min, indicating that this chemosensor can be used for real-time tracing of Cu^{2+} in a test system. DFT calculations provided an optimized structure of L–Cu^{2+}, the frontier orbitals of **L** and L–Cu^{2+}, contributions of specific electronic transitions to the molecular orbital transitions, electronic energies and Cartesian coordinates of L–Cu^{2+}. These calculated results verified the 1:1 binding mode between **L** and Cu^{2+}. The corresponding quenching mechanism appeared to involve charge transfer from the excited ampyrone moiety to the region surrounding the Cu^{2+} ion, and thus provided a pathway for nonradiative deactivation of the excited state. Furthermore, this sensing system was further successfully applied to fluorescent cell imaging, hence, the chemsensor had potential applications in physiological and environmental systems for the detection of Cu^{2+} and the result was of great significance for the development of molecular recognition systems.

Acknowledgments

This work was financially supported by the National Natural Scientific Foundation of China (Nos. 21201092 and 209237057), the Research Fund for the Doctoral Program of Higher Education (20120211120020), the Gansu NST (1208RJYA028) and the Fundamental Research Funds for the Central Universities (lzujbky-2013-194).

Appendix A. Supplementary materials

Supplementary materials associated with this article can be found in the online version at http://dx.doi.org/10.1016/j.talanta.2014.02.034.

References

[1] (a) A.P.D. Silva, H.Q.N. Gunaratne, T. Gunnlaugsson, A.J.M. Huxley, C.P. McCoy, J.T. Rademacher, Chem. Rev. 97 (1997) 1515–1566;
(b) H.S. Jung, P.S. Kwon, J.W. Lee, J.I. Kim, C.S. Hong, J.W. Kim, S.H. Yan, J.Y. Lee, J.H. Lee, T.H. Joo, J.S. Kim, J. Am. Chem. Soc. 131 (2009) 2008–2012.
[2] (a) C.Y. Lai, B.G. Trewyn, D.M. Jeftinija, K. Jeftinija, S. Xu, S. Jeftinija, V.S.Y. Lin, J. Am. Chem. Soc. 125 (2003) 4451–4459;
(b) M. Numata, C. Li, A.H. Bae, K. Kaneko, K. Sakurai, S. Shinkai, Chem. Commun. 37 (2005) 4655–4657.
[3] (a) H.N. Kim, M.H. Lee, H.J. Kim, J.S. Kim, J. Yoon, Chem. Soc. Rev. 37 (2008) 1465–1472;
(b) E.L. Que, D.W. Domaille, C.J. Chang, Chem. Rev. 108 (2008) 1517–1549.
[4] (a) X.Q. Chen, S.W. Nam, M.J. Jou, Y. Kim, S.J. Kim, S. Park, J. Yoon, Org. Lett. 10 (2008) 5235–5238;
(b) J.S. Wu, I.C. Hwang, K.S. Kim, J.S. Kim, Org. Lett. 9 (2007) 907–910;
(c) M. Suresh, S. Mishra, S.K. Mishra, E. Suresh, A.K. Mandal, A. Shrivastav, A. D. Resonance, Org. Lett. 11 (2009) 2740–2743.
[5] (a) E.M. Nolan, J. Jaworski, K.I. Okamoto, Y. Hayashi, M. Sheng, S.J. Lippard, J. Am. Chem. Soc. 127 (2005) 16812–16823;
(b) C.C. Woodroofe, S.J. Lippard, J. Am. Chem. Soc. 125 (2003) 11458–11459.
[6] (a) Y. Xiang, A. Tong, P. Jin, Y. Ju, Org. Lett. 8 (2006) 2863–2866;
(b) M. Royzen, Z. Dai, J.W. Canary, J. Am. Chem. Soc. 127 (2005) 1612–1613;
(c) L. Huang, X. Wang, G. Xie, P. Xi, Z. Li, M. Xu, Y. Wu, D. Bai, Z. Zeng, Dalton Trans. 39 (2010) 7894–7896.
[7] P. Xi, L. Huang, G. Xie, F. Chen, Z. Xu, D. Bai, Z. Zeng, Dalton Trans. 40 (2011) 6382–6384.
[8] G. Muthaup, A. Schlicksupp, L. Hess, D. Beher, T. Ruppert, C.L. Masters, K. Beyreuther, Science 271 (1996) 1406–1409.
[9] (a) Y. Wang, L. Wang, L. Shi, Z. Shang, W. Jin, Talanta 94 (2012) 172–177;
(b) Y.Q. Weng, F. Yue, Y.R. Zhong, B.H. Ye, Inorg. Chem. 46 (2007) 7749–7755;
(c) L. Zeng, E.W. Miller, A. Pralle, E.Y. Isacoff, C.J. Chang, J. Am. Chem. Soc. 128 (2006) 10–11;
(d) Y. Xiang., Z. Li, X. Chen, A. Tong, Talanta 74 (2008) 1148–1153;
(e) Z. Xu, X. Qian, J. Cui, Org. Lett. 7 (2005) 3029–3032;
(f) T. Noipa, T. Tuntulani, W. Ngeontae, Talanta 105 (2013) 320–326.
[10] M. Royzen, Z. Dai, J.W. Canary, J. Am. Chem. Soc. 127 (2005) 1612–1613.
[11] (a) M.C.Y. Chang, A. Pralle, E.Y. Isacoff, C.J. Chang, J. Am. Chem. Soc. 126 (2004) 15392–15393;
(b) X. Peng, J. Du, J. Fan, J. Wang, Y. Wu, J. Zhao, S. Sun, T. Xu, J. Am. Chem. Soc. 129 (2007) 1500–1501.
[12] L. Huang, J. Cheng, K. Xie, P. Xi, F. Hou, Z. Li, G. Xie, Y. Shi, H. Liu, D. Bai, Z. Zeng, Dalton Trans. 40 (2011) 10815–10817.
[13] Z. Li, Q.Y. Chen, P.D. Wang, Y. Wu, RSC Adv. 3 (2013) 5524–5528.
[14] G. Sivaraman, T. Anand, D. Chellappa, RSC Adv. 3 (2013) 17029–17033.
[15] J. Zhang, B. Zhao, C. Li, X. Zhu, R. Qiao, Sensors Actuators B, ⟨http://10.1016/j.snb.2014.01.116⟩.
[16] H.S. Jung, P.S. Kwon, J.W. Lee, J. Kim, C.S. Hong, J.W. Kim, S. Yan, J.Y. Lee, J.H. Lee, T. Joo, J.S. Kim, J. Am. Chem. Soc. 131 (2009) 2008–2012.